ELECTRON TRANSMISSION THROUGH GRAPHENE MONOLAYER-BILAYER JUNCTION: AN ANALYTICAL APPROACH

J. Ruseckas [a], A. Mekys [a], G. Juzeliūnas [a, b], and I. V. Zozoulenko [c]

[a] *Institute of Theoretical Physics and Astronomy, Vilnius University, A. Goštauto 12, LT-01108 Vilnius,*
Lithuania
E-mail: algirdas.merkys@ff.vu.lt

[b] *Lithuanian University of Educational Sciences, Studentų 39, LT-08106 Vilnius, Lithuania*

[c] *Solid State Electronics, ITN, Linköping University, 601 74 Norköping, Sweden*

A junction of monolayer and bilayer graphene nanoribbons is investigated using the tight-binding approximation. An external potential is applied on the bilayer graphene layers to control the electronic transport properties of the junction. The reflection and transmission probabilities for an incident electron at the junction are analytically calculated. The dependence of the reflection probability on the external potential, the wave vector of the incident electron and the width of the nanoribbon are evaluated.

Keywords: graphene, electron transmission

PACS: 81.05.ue

1. Introduction

Graphene is a single sheet of carbon atoms arranged in a honeycomb lattice. Despite being a composition part of graphite, a carbon form known for a long time, graphene was isolated only in 2004. Graphene has attracted scientific interest because of its unusual electronic and transport properties that are strikingly different from those of conventional semiconductor-based two-dimensional electronic systems (for a review see Refs. [1–4]). The potential impact of this new material on electronics was immediately recognised. It has been demonstrated that graphene has the highest carrier mobility at room temperature in comparison to any other material [5]. However, graphene is a semi-metal with no energy gap and zero density of states at the Fermi energy. This makes it difficult to utilise it in electronic devices such as field effect transistor (FET) requiring a large on/off current ratio. The energy gap can be opened in bilayer graphene by applying a gate

voltage between the layers [6]. This gate-induced band-gap was demonstrated by Oostinga et al. [7], and the on/off current ratio of around 100 at room temperature for a dual-gate bilayer graphene FET was reported by IBM [8].

Structures consisting of graphene and bilayer graphene parts can be created by a simple overlapping of one sheet of graphene over the other. The simplest possible structure containing graphene and bilayer graphene is a junction of these two materials. Due to asymmetry such junction may function in a similar manner to diode because the conditions for the electron to pass the junction from the different sides are not the same. The symmetric structure with two opposite junctions (graphene-bilayer graphene-graphene) has been already investigated in [9] using continuum approximation when energy is close to the Dirac point. External voltage was applied to control the electronic transport parameters of the structure. Similar structures with more different edge geometries were

investigated in [10]. The investigation was also limited to the continuum approximation without application of the external voltage. In our work we use the tight-binding approximation, which allows us to investigate the system properties for the whole energy range. The deficiency of the tight-binding approximation is the neglect of higher order corrections, which include the graphene nanoribbon (GNR) bending effect or its conversion into the nanotube. In this way it becomes indistinguishable if we have an infinite nanotube with a semi-infinite nanotube inside or an infinite nanotube is inserted into another semi-infinite nanotube.

An additional insight into electronic properties of graphene and GNRs can be obtained from exact analytical approaches. Analytic calculations for the electronic structure of the GNRs have been reported in Refs. [11–15]. The electronic structure of bilayer graphene was addressed in Refs. [16–20] where the analytical results were presented (both exact and perturbative). The electronic structure of bilayer GNRs was analytically obtained in [21]. A numerical study of the magnetobandstructure of the GNRs was reported in Ref. [22, 23], and the numerical treatment of the edge states in the bilayer GNRs was presented in Ref. [20]. The aim of the present study is to provide an exact analytical description of the π electron reflection and transmission in the junction of the bilayer and monolayer nanoribbons with armchair edges, with applied external potential.

The paper is organised as follows: in Sec. 2 we present the known analytical results of monolayer and bilayer graphene and construct the wave function for the junction. Subsequently in Sec. 3 we analyse the properties of the electronic transmission through the junction. Finally, Sec. 4 summarises our findings.

2. Analytical expressions of the electronic states at the junction

Analytical expressions for the electron spectrum in GNRs and graphene nanotubes (GNTs), based on a tight-binding model, were provided in Ref. [14] and the expressions for bilayer graphene were provided in Ref. [21]. In this section we exploit these expressions to construct the wave function for the system of graphene connected to bilayer graphene. One may consider this system as a single infinite length graphene ribbon with another semi-infinite graphene ribbon overlapping, but mathematically it is simpler to consider the system as a junction of semi-infinite graphene with semi-infinite bilayer graphene ribbons. For simplicity, we analyse in this work only AB-α stacking of bilayer graphene, as shown in Fig. 1, and other configurations are left for the future calculations. Also, the atoms at the junction edge are arranged in a zigzag configuration, while the sides of the ribbon are in the armchair configuration of the atoms.

We consider π electron spectrum in an infinite sheet of graphene. The structure of graphene can be viewed as a hexagonal lattice with a basis of two
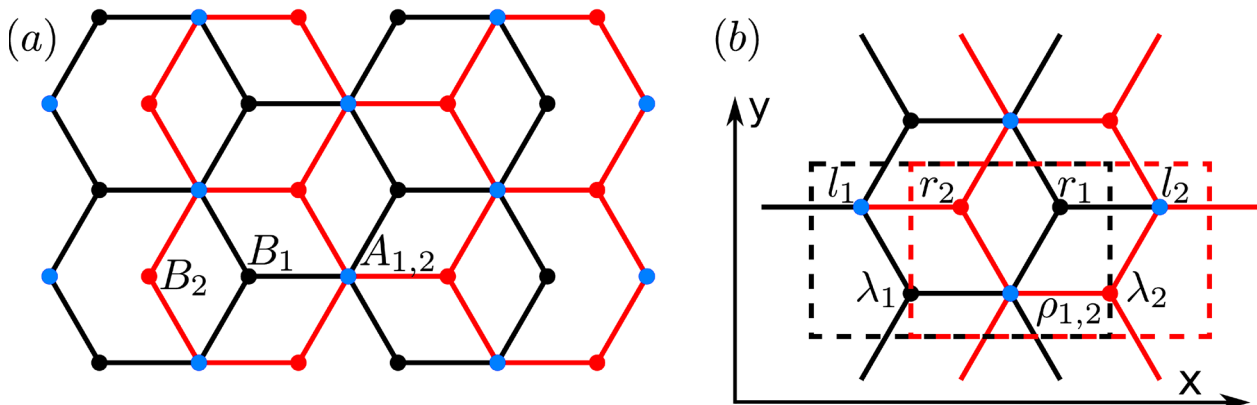

Fig. 1. (Colour online) (a) Sub-lattices A_1, A_2, B_1, B_2 on bilayer graphene in AB-α stacking. (b) Indication of labels of carbon atom cells used for bilayer graphene.

atoms per unit cell. The Cartesian components of the lattice vectors $\mathbf{a}_1$ and $\mathbf{a}_2$ are $a(\sqrt[3]{2}, \sqrt[3]{2})$ and $a(\sqrt[3]{2}, -\sqrt[3]{2})$, respectively. Here $a \approx 1.42$ is the carbon-carbon distance [1]. The three nearest-neighbour vectors are given by $\delta_1 = a(\frac{1}{2}, \sqrt[3]{2})$, $\delta_2 = a(\frac{1}{2}, -\sqrt[3]{2})$, and $\delta_3 = a(-1,0)$. The tight-binding Hamiltonian for electrons in graphene has the form

$$H_{\mathrm{gr}} = -t \sum_{\langle i,j \rangle} (a_i^\dagger b_j + b_j^\dagger a_i), \tag{1}$$

where the operators a_i and b_i annihilate an electron on sub-lattice A at site $\boldsymbol{R}_i^A$ and on sub-lattice B at site $\boldsymbol{R}_i^B$, respectively (for single graphene consider Fig. 1 with $A_1 = A$ and $B_1 = B$). The parameter t is the nearest-neighbour hopping energy ($t \approx 2.8$ eV). Hereinafter all energies will be written in the units of the hopping integral t, therefore we set $t = 1$. Let us label the elementary cells of the lattice with two numbers p and q. Then the atoms in the sub-lattices A and B are positioned at $\mathbf{R}_{p,q}^A = p\mathbf{a}_1 + q\mathbf{a}_2$ and $\mathbf{R}_{p,q}^B = \delta_1 + p\mathbf{a}_1 + q\mathbf{a}_2$ respectively.

The π electron wave function satisfies the Schrödinger equation

$$H\Psi = E\Psi. \tag{2}$$

We search for the eigenvectors of the Hamiltonian (1) in the form of the plane waves (Bloch states) by taking the probability amplitudes to find an atom in the sites $\mathbf{R}_{p,q}^A$ and $\mathbf{R}_{p,q}^B$ of the sub-lattices A and B as

$$\psi_{p,q}^A = c^A e^{i\mathbf{k}\cdot\mathbf{R}_{p,q}^A}, \quad \psi_{p,q}^B = c^B e^{i\mathbf{k}\cdot\mathbf{R}_{p,q}^B}. \tag{3}$$

Thus Eq. (2) yields the eigenvalue equations for the coefficients c^A and c^B (envelope functions):

$$-Ec^A = c^B \tilde{\phi}(\mathbf{k}), \tag{4}$$

$$-Ec^B = c^A \tilde{\phi}(-\mathbf{k}), \tag{5}$$

where

$$\tilde{\phi}(\mathbf{k}) \equiv e^{i\mathbf{k}\cdot\delta_1} + e^{i\mathbf{k}\cdot\delta_2} + e^{i\mathbf{k}\cdot\delta_3}. \tag{6}$$

Further we will consider the spectrum of π electrons in an infinite sheet of bilayer graphene. The tight-binding Hamiltonian for electrons in bilayer graphene has the following form:

$$H_{\mathrm{bi}} = V \sum_j (a_{j,2}^\dagger a_{j,2} + b_{j,2}^\dagger b_{j,2} - a_{j,1}^\dagger a_{j,1} - b_{j,1}^\dagger b_{j,1})$$

$$-t \sum_{\langle i,j \rangle, p} (a_{i,p}^\dagger b_{j,p} + b_{j,p}^\dagger a_{i,p}) - t_\perp \sum_j (a_{j,1}^\dagger a_{j,2} + a_{j,2}^\dagger a_{j,1}), \tag{7}$$

where the operators $a_{i,p}$ and $b_{i,p}$ annihilate an electron on sub-lattice A_p at site $\mathbf{R}_i^{A_p}$ and on sub-lattice B_p at site $\mathbf{R}_i^{B_p}$ respectively (Fig. 1). The index $p = 1,2$ numbers the layers in the bilayer system. In the Hamiltonian (7) we neglected the terms corresponding to the hopping between atom B_1 and atom B_2, with the hopping energy γ_3, and the terms corresponding to the hopping between atom A_1 (A_2) and atom B_2 (B_1) with the hopping energy γ_4. The neglect of these hopping terms leads to the minimal model of bilayer graphene [19]. The parameter $t_\perp$ ($t_\perp \approx 0.4$ eV) is the hopping energy between atom A_1 and atom A_2 while V is half the shift in the electro-chemical potential between the two layers. Similarly as in monolayer graphene, we express all the energies in the units of t. The atoms in the sub-lattices A_1 and A_2 are positioned at $\mathbf{R}_{p,q}^{A\,1,2} = p\mathbf{a}_1 + q\mathbf{a}_2$, in the sub-lattice B_1 the aptoms are positioned at $\mathbf{R}_{p,q}^{B\,1} = \delta_1 + p\mathbf{a}_1 + q\mathbf{a}_2$ and in the sub-lattice B_2 the atoms are positioned at $\mathbf{R}_{p,q}^{B\,2} = -\delta_1 + p\mathbf{a}_1 + q\mathbf{a}_2$. We search for the eigenvectors of the Hamiltonian (7) in the form of the plane waves. The probability amplitudes to find an atom in the sites $\mathbf{R}_{p,q}^{A\,1,2}$ and $\mathbf{R}_{p,q}^{B\,1,2}$ of the sub-lattices A_j and A_j are:

$$\psi_{p,q}^{A_{1,2}} = c^{A_{1,2}} e^{i\mathbf{k}\cdot\mathbf{R}_{p,q}^{A_{1,2}}}, \quad \psi_{p,q}^{B_{1,2}} = c^{B_{1,2}} e^{i\mathbf{k}\cdot\mathbf{R}_{p,q}^{B_{1,2}}}. \tag{8}$$

The coefficients (envelope functions) c^{A_p} and c^{B_p} obey the eigenvalue equations:

$$-Ec^{A_1} = Vc^{A_1} + c^{B_1}\tilde{\phi}(\mathbf{k}) + \gamma c^{A_2}, \tag{9}$$

$$-Ec^{B_1} = Vc^{B_1} + c^{A_1}\tilde{\phi}(-\mathbf{k}), \tag{10}$$

$$-Ec^{A_2} = -Vc^{A_2} + c^{B_2}\tilde{\phi}(-\mathbf{k}) + \gamma c^{A_1}, \tag{11}$$

$$-Ec^{B_2} = -Vc^{B_2} + c^{A_2}\tilde{\phi}(\mathbf{k}). \tag{12}$$

Here energy E, potential V, and interaction between layers $\gamma \equiv t_\perp/t$ are in the units of the hopping integral t. Using the nearest-neighbour hopping energy $t \approx 2.8$ eV and the hopping energy between two layers $t_\perp \approx 0.4$ eV, one gets $\gamma \approx 0.14$.

2.1. Electron spectrum in the infinite sheet of graphene

Since we are interested in configurations of graphene with rectangular geometry, we use a rectangular unit cell as in Ref. [14] and follow the names of the variables and functions used in Ref. [21]. Such unit cell has four atoms labelled with symbols l, λ, ρ, r, as shown in Fig. 1 (consider at this point only one layer with the labels l_1, λ_1, ρ_1, r_1, A_1, B_1).

The atoms with labels l and ρ belong to the sub-lattice A, the atoms with labels λ and r belong to the sub-lattice B. The position of the unit cell is indicated with two numbers, n and m. The first Brillouin zone corresponding to the rectangular unit cell contains the values of the wave vectors κ, ξ. The eigenvectors describing the system have the form of plane waves:

$$\psi^{m,n,\alpha}(\kappa, \xi) = c_\alpha(\kappa, \xi) e^{i\xi m + i\kappa}, \tag{13}$$

where $\alpha = l, \rho, \lambda, r$.

The coefficients of the eigenvectors are:

$$c_r = 1, \qquad c_\rho = -e^{-i\frac{\xi}{2}} \frac{\phi(\kappa,\xi)}{E(\kappa,\xi)}, \tag{14}$$

$$c_l = -s_3 e^{-i\frac{\kappa}{2}} \frac{\phi(\kappa,\xi)}{E(\kappa,\xi)}, \qquad c_\lambda = s_3 e^{-i\frac{1}{2}(\kappa+\xi)}, \tag{15}$$

where

$$\phi(\kappa,\xi) = s_3 e^{-i\frac{\kappa}{2}} + 2\cos\left(\frac{\xi}{2}\right) \tag{16}$$

and $s_3 = \pm 1$ indicates the dispersion branches that appear due to a smaller Brillouin zone (for more details see Ref. [21]). The energy is (with $s_1 = \pm 1$):

$$E(\kappa,\xi) = s_1 \sqrt{1 + 4\cos^2\left(\frac{\xi}{2}\right) + s_3 4\cos\left(\frac{\xi}{2}\right)\cos\left(\frac{\kappa}{2}\right)}. \tag{17}$$

The zero energy points have coordinates $\left(0, \pm\frac{2\pi}{3}\right)$ in the Brillouin zone corresponding to the rectangular unit cell.

Since we consider finite-size graphene sheets, evanescent solutions become important. We assume that exponentially decreasing or increasing solution can be obtained by taking $\kappa = i|\kappa|$ or $\xi = i|\xi|$ in Eqs. (14), (15) and (17).

2.2. Electron spectrum in the infinite sheet of bilayer graphene

The form of the wave function is similar to monolayer graphene, Eq. (13), only the labels change:

$$\psi_{m,n,\alpha_p}(\kappa, \xi) = c_{\alpha_p}(\kappa, \xi) e^{i\xi m + i\kappa n}, \tag{18}$$

Here the label $p = 1, 2$ is the number of the layer. The coefficients of the eigenvectors are (from Ref. [21]):

$$c_{r_1} = 1, \qquad c_{\rho_1} = -e^{-i\frac{\xi}{2}} \frac{E(\kappa,\xi)+V}{\phi(-\kappa,\xi)}, \tag{19}$$

$$c_{l_1} = -s_3 e^{-i\frac{\kappa}{2}} \frac{E(\kappa,\xi)+V}{\phi(-\kappa,\xi)}, \qquad c_{\lambda_1} = s_3 e^{-i\frac{1}{2}(\kappa+\xi)}, \tag{20}$$

$$c_{r_2} = -\frac{\phi(\kappa,\xi)}{\phi(-\kappa,\xi)} f(\kappa,\xi),$$

$$c_{\rho_2} = s_1 s_2 e^{-i\frac{\xi}{2}} \frac{E(\kappa,\xi)-V}{\phi(-\kappa,\xi)} f(\kappa,\xi), \tag{21}$$

$$c_{l_2} = s_3 e^{i\frac{\kappa}{2}} \frac{E(\kappa,\xi)-V}{\phi(-\kappa,\xi)} f(\kappa,\xi),$$

$$c_{\lambda_2} = -s_3 e^{i\frac{1}{2}(\kappa-\xi)} \frac{\phi(\kappa,\xi)}{\phi(-\kappa,\xi)} f(\kappa,\xi). \tag{22}$$

Here $s_1, s_2 = \pm 1$ are the sign coefficients:

$$f(\kappa,\xi) = \frac{(E(\kappa,\xi)+V)^2 - |\phi(\kappa,\xi)|^2}{\gamma(E(\kappa,\xi)-V)}, \tag{23}$$

and the expression for energy is

$$E(\kappa,\xi) = s_1 \left[\frac{\gamma^2}{2} + V^2 + |\phi(\kappa,\xi)|^2 \right.$$

$$\left. + s_2 \sqrt{\frac{\gamma^4}{4} + |\phi(\kappa,\xi)|^2 (4V^2 + \gamma^2)} \right]^{\frac{1}{2}}. \quad (24)$$

The function $\phi(\kappa, \xi)$ has the same expression as Eq. (16), and V is the electrostatic potential applied on one layer of bilayer graphene, while $-V$ is applied on the other. The parameter γ describes the interaction between the layers in bilayer graphene, $\gamma = 0.14$, measured in the same units as energy.

In bilayer graphene there are two eigenstates with wave vectors $\kappa^{(1)}$ and $\kappa^{(2)}$, having different absolute values but corresponding to the same energy: $E(\kappa^{(1)}, \xi) = E(\kappa^{(2)}, \xi)$. One or both of the wave vectors $\kappa^{(1)}$, $\kappa^{(2)}$ can be imaginary. The energy can be equal only if the signs s_1, s_2 obey the condition

$$s_1^{(2)} s_2^{(2)} = -s_1^{(1)} s_2^{(1)}. \quad (25)$$

It has to be noted that the sign coefficients from the set s_1, s_2, s_3 in bilayer graphene are not necessary, the same as in the single graphene equations.

In addition to the propagating waves, for finite-size bilayer graphene sheets evanescent solutions become important. We assume that exponentially decreasing or increasing solution can be obtained by taking $\kappa = i|\kappa|$ or $\xi = i|\xi|$. In addition to the purely imaginary ξ there are solutions, corresponding to $s_3 = -1$, having complex values of ξ.

2.3. Calculation of wave vector from energy

From the dispersion of bilayer graphene (Eq. (24)) we obtain

$$E^2 - \frac{\gamma^2}{2} - V^2 - |\phi|^2 = s_2 \sqrt{\frac{\gamma^4}{4} + |\phi|^2 (4V^2 + \gamma^2)}. \quad (26)$$

From this dispersion equation we find the expression for $|\phi|^2$:

$$|\phi|^2 = (E^2 + V^2) \pm \sqrt{E^2(4V^2 + \gamma^2) - V^2\gamma^2}. \quad (27)$$

It should be noted that when

$$E^2 < \frac{V^2\gamma^2}{4V^2 + \gamma^2},$$

we get that $|\phi|^2$ is a complex number. This means that κ is also a complex number and has both real and imaginary parts.

We have that

$$|\phi|^2 = 1 + 4\cos^2\left(\frac{\xi}{2}\right) + s_3 4 \cos\left(\frac{\xi}{2}\right) \cos\left(\frac{\kappa}{2}\right); \quad (28)$$

therefore, the dimesnionless x-component of the wave vector κ can be expressed as

$$\kappa = 2\arccos\left[s_3 \frac{|\phi|^2 - 1}{4\cos\left(\frac{\xi}{2}\right)} - s_3 \cos\left(\frac{\xi}{2}\right) \right]. \quad (29)$$

The indices s_1 and s_1 can be calculated from the equations (derived from Eq. (26))

$$s_2 = \frac{E^2 - \left(\frac{\gamma^2}{2} + V^2 + |\phi|^2 \right)}{\sqrt{\frac{\gamma^4}{4} + |\phi|^2 (4V^2 + \gamma^2)}} \quad (30)$$

and

$$s_1 = \frac{E}{\sqrt{\frac{\gamma^2}{2} + V^2 + |\phi|^2 + s_2 \sqrt{\frac{\gamma^4}{4} + |\phi|^2 (4V^2 + \gamma^2)}}}. \quad (31)$$

2.4. Construction of wave functions for the junction

The graphene and bilayer graphene junction is constructed as shown in Fig. 2. The unit cells (indicated with two numbers n and m) are the same both for graphene and bilayer graphene, just starting at a certain cell n (we choose: $n < 0$) the upper layer
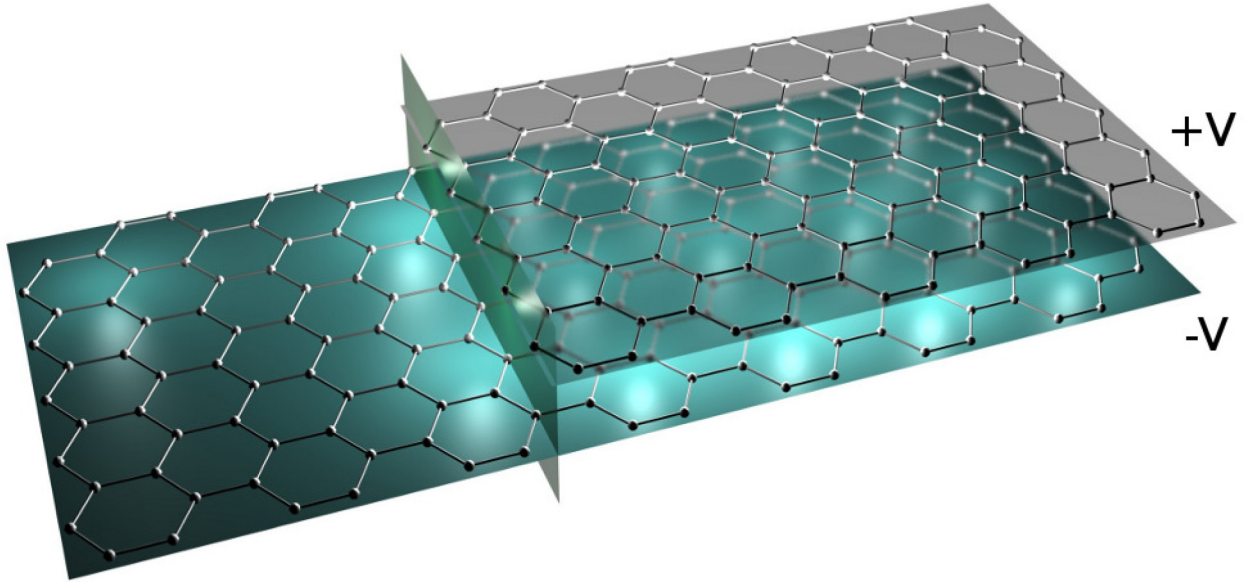
Fig. 2. (Colour online) Perspective view of the graphene-bilayer graphene junction. The upper layer is connected to the potential +V, while the lower layer to the potential –V.

of bilayer graphene is removed. Mathematically the condition for the absence of the second layer is:

$$\psi_{m,n,\alpha_2}(\kappa, \xi) = 0, \qquad n < 0. \tag{32}$$

In particular, at the boundary

$$\psi_{m,-1,l_2}(\kappa, \xi) = 0. \tag{33}$$

The condition for connecting monolayer graphene and bilayer graphene solutions is that amplitudes of monolayer and bilayer graphene should coincide:

$$\psi_{m,0,\lambda}(\kappa, \xi) = \psi_{m,0,\lambda_1}(\kappa, \xi), \tag{34}$$

$$\psi_{m,0,l}(\kappa, \xi) = \psi_{m,0,l_1}(\kappa, \xi). \tag{35}$$

We analyse the situation when the electron approaches the junction from the graphene side and is partially reflected with the reflection probability $|R|^2$. The incoming electron wave vector component κ brings the phase $e^{i\kappa n}$, while back reflected it is $e^{-i\kappa n}$. Since the system is symmetric in the transverse direction, we construct the combinations for the wave vector component ξ in the form $\left(c_\alpha(\xi, \kappa)e^{i\xi_j m} - c_\alpha(-\xi, \kappa)e^{-i\xi_j m}\right)$. Here ξ has the index j for the general case when the discrete values of ξ are used to describe the finite size system.

The form of the solution in monolayer graphene then is:

$$\psi_{m,n,\alpha}(\kappa, \xi) = [c_\alpha(\xi, \kappa)e^{i\xi_j m} - c_\alpha(-\xi, \kappa)e^{-i\xi_j m}]e^{i\kappa n}$$

$$+ R[c_\alpha(\xi, -\kappa)e^{i\xi_j m} - c_\alpha(-\xi, -\kappa)e^{-i\xi_j m}]e^{-i\kappa n}. \tag{36}$$

In bilayer graphene there are two wave vectors $\kappa^{(1)}$, $\kappa^{(2)}$ corresponding to the same energy, thus we introduce two coefficients T_1 and T_2. The form of the solution in bilayer graphene is:

$$\psi_{m,n,\alpha_p}(\kappa, \xi) = T_1[c_{\alpha_p}(\xi, \kappa^{(1)})e^{i\xi_j m} - c_{\alpha_p}(-\xi, \kappa^{(1)})e^{-i\xi_j m}]e^{i\kappa^{(1)} n}$$

$$+ T_2[c_{\alpha_p}(\xi, \kappa^{(2)})e^{i\xi_j m} - c_{\alpha_p}(-\xi, -\kappa^{(2)})e^{-i\xi_j m}]e^{-i\kappa^{(2)} n}. \tag{37}$$

From the boundary conditions (Eqs. (33)–(35)) we obtain three equations for three unknowns (R, T_1 and T_2).

2.5. Reflection and transmission amplitudes for V = 0

In the case when the external potential is zero, $V = 0$, by inserting the expressions for the coefficients from Eqs. (14), (15) and (19)–(22) we get:

$$T_1 \frac{s_3^{(1)} \mathrm{e}^{-\mathrm{i}\frac{\kappa^{(1)}}{2}}}{\phi(-\kappa^{(1)},\xi_j)} - T_2 \frac{s_3^{(2)} \mathrm{e}^{-\mathrm{i}\frac{\kappa^{(2)}}{2}}}{\phi(-\kappa^{(2)},\xi_j)} = 0, \qquad (38)$$

$$s_3 \mathrm{e}^{-\mathrm{i}\frac{\kappa}{2}} + R s_3 \mathrm{e}^{\mathrm{i}\frac{\kappa}{2}} = T_1 s_3^{(1)} \mathrm{e}^{-\mathrm{i}\frac{\kappa^{(1)}}{2}} + T_2 s_3^{(2)} \mathrm{e}^{-\mathrm{i}\frac{\kappa^{(2)}}{2}}, \quad (39)$$

$$\frac{s_3 \mathrm{e}^{-\mathrm{i}\frac{\kappa}{2}}}{\phi(-\kappa,\xi_j)} + R \frac{s_3 \mathrm{e}^{\mathrm{i}\frac{\kappa}{2}}}{\phi(\kappa,\xi_j)} =$$

$$T_1 \frac{s_3^{(1)} \mathrm{e}^{-\mathrm{i}\frac{\kappa^{(1)}}{2}}}{\phi(-\kappa^{(1)},\xi_j)} + T_2 \frac{s_3^{(2)} \mathrm{e}^{-\mathrm{i}\frac{\kappa^{(2)}}{2}}}{\phi(-\kappa^{(2)},\xi_j)}. \qquad (40)$$

The solutions are:

$$R = -\mathrm{e}^{-\mathrm{i}\kappa} \frac{\phi(\kappa,\xi_j)}{\phi(-\kappa,\xi_j)} \frac{s_3^{(1)} \mathrm{e}^{\mathrm{i}\frac{\kappa^{(1)}}{2}} + s_3^{(2)} \mathrm{e}^{\mathrm{i}\frac{\kappa^{(2)}}{2}} - 2s_3 \mathrm{e}^{\mathrm{i}\frac{\kappa}{2}}}{s_3^{(1)} \mathrm{e}^{\mathrm{i}\frac{\kappa^{(1)}}{2}} + s_3^{(2)} \mathrm{e}^{\mathrm{i}\frac{\kappa^{(2)}}{2}} - 2s_3 \mathrm{e}^{-\mathrm{i}\frac{\kappa}{2}}}, (41)$$

$$T_1 = \frac{\phi(-\kappa^{(1)},\xi_j)}{\phi(-\kappa,\xi_j)} \frac{2\mathrm{i} \sin\left(\frac{\kappa}{2}\right) s_3^{(1)} \mathrm{e}^{\frac{\mathrm{i}}{2}(\kappa^{(1)}-\kappa)}}{s_3^{(1)} \mathrm{e}^{\mathrm{i}\frac{\kappa^{(1)}}{2}} + s_3^{(2)} \mathrm{e}^{\mathrm{i}\frac{\kappa^{(2)}}{2}} - 2s_3 \mathrm{e}^{-\mathrm{i}\frac{\kappa}{2}}}, (42)$$

$$T_2 = \frac{\phi(-\kappa^{(2)},\xi_j)}{\phi(-\kappa,\xi_j)} \frac{2\mathrm{i} \sin\left(\frac{\kappa}{2}\right) s_3^{(2)} \mathrm{e}^{\frac{\mathrm{i}}{2}(\kappa^{(2)}-\kappa)}}{s_3^{(1)} \mathrm{e}^{\mathrm{i}\frac{\kappa^{(1)}}{2}} + s_3^{(2)} \mathrm{e}^{\mathrm{i}\frac{\kappa^{(2)}}{2}} - 2s_3 \mathrm{e}^{-\mathrm{i}\frac{\kappa}{2}}}. (43)$$

2.6. Reflection and transmission amplitudes for V > 0

With the potential $-V$ the coefficients of the eigen-vectors in graphene are (Ref. [21]):

$$c_r = 1, \qquad c_\rho = -\mathrm{e}^{-\mathrm{i}\frac{\xi}{2}} \frac{E(\kappa,\xi) + V}{\phi(-\kappa,\xi)}, \qquad (44)$$

$$c_l = -s_3 \mathrm{e}^{-\mathrm{i}\frac{\kappa}{2}} \frac{E(\kappa,\xi) + V}{\phi(-\kappa,\xi)}, \qquad c_\lambda = s_3 \mathrm{e}^{-\mathrm{i}\frac{1}{2}(\kappa+\xi)}. (45)$$

By inserting the expressions for the coefficients from Eqs. (44), (45) and (19)–(22) into boundary conditions we get the equations:

$$T_1 \frac{s_3^{(1)} f(\kappa^{(1)},\xi_j) \mathrm{e}^{-\mathrm{i}\frac{\kappa^{(1)}}{2}}}{\phi(-\kappa^{(1)},\xi_j)} + T_2 \frac{s_3^{(2)} f(\kappa^{(2)},\xi_j) \mathrm{e}^{-\mathrm{i}\frac{\kappa^{(2)}}{2}}}{\phi(-\kappa^{(2)},\xi_j)} = 0, (46)$$

$$s_3 \mathrm{e}^{-\mathrm{i}\frac{\kappa}{2}} + R s_3 \mathrm{e}^{\mathrm{i}\frac{\kappa}{2}} = T_1 s_3^{(1)} \mathrm{e}^{-\mathrm{i}\frac{\kappa^{(1)}}{2}} + T_2 s_3^{(2)} \mathrm{e}^{-\mathrm{i}\frac{\kappa^{(2)}}{2}}, \quad (47)$$

$$\frac{s_3 \mathrm{e}^{-\mathrm{i}\frac{\kappa}{2}}}{\phi(-\kappa,\xi_j)} + R \frac{s_3 \mathrm{e}^{\mathrm{i}\frac{\kappa}{2}}}{\phi(\kappa,\xi_j)} =$$

$$T_1 \frac{s_3^{(1)} \mathrm{e}^{-\mathrm{i}\frac{\kappa^{(1)}}{2}}}{\phi(-\kappa^{(1)},\xi_j)} + T_2 \frac{s_3^{(2)} \mathrm{e}^{-\mathrm{i}\frac{\kappa^{(2)}}{2}}}{\phi(-\kappa^{(2)},\xi_j)}. \qquad (48)$$

The solutions for these equations are

$$R = -\mathrm{e}^{-\mathrm{i}\kappa} \frac{\phi(\kappa,\xi_j)}{\phi(-\kappa,\xi_j)} \left[F(\kappa^{(1)}, \kappa^{(2)},\xi_j) \right.$$

$$\times \left(s_3^{(2)} \mathrm{e}^{\mathrm{i}\frac{\kappa^{(2)}}{2}} - s_3 \mathrm{e}^{\mathrm{i}\frac{\kappa}{2}} \right) - s_3^{(1)} \mathrm{e}^{\mathrm{i}\frac{\kappa^{(1)}}{2}} + s_3 \mathrm{e}^{\mathrm{i}\frac{\kappa}{2}} \right]$$

$$\times \left[F(\kappa^{(1)},\kappa^{(2)},\xi_j) \left(s_3^{(2)} \mathrm{e}^{\mathrm{i}\frac{\kappa^{(2)}}{2}} - s_3 \mathrm{e}^{-\mathrm{i}\frac{\kappa}{2}} \right) \right.$$

$$\left. - s_3^{(1)} \mathrm{e}^{\mathrm{i}\frac{\kappa^{(1)}}{2}} + s_3 \mathrm{e}^{-\mathrm{i}\frac{\kappa}{2}} \right]^{-1}, \qquad (49)$$

$$T_1 = \frac{\phi(-\kappa^{(1)},\xi_j)}{\phi(-\kappa,\xi_j)} \left[-2\mathrm{i}s_3^{(1)} \mathrm{e}^{\frac{\mathrm{i}}{2}(\kappa^{(1)}-\kappa)} \sin\left(\frac{\kappa}{2}\right) \right]$$

$$\times \left[F(\kappa^{(1)},\kappa^{(2)},\xi_j) \left(s_3^{(2)} \mathrm{e}^{\mathrm{i}\frac{\kappa^{(2)}}{2}} - s_3 \mathrm{e}^{-\mathrm{i}\frac{\kappa}{2}} \right) \right.$$

$$\left. - s_3^{(1)} \mathrm{e}^{\mathrm{i}\frac{\kappa^{(1)}}{2}} + s_3 \mathrm{e}^{-\mathrm{i}\frac{\kappa}{2}} \right]^{-1}, \qquad (50)$$

$$T_2 = \frac{\phi(-\kappa^{(2)},\xi_j)}{\phi(-\kappa,\xi_j)} \left[2\mathrm{i}s_3^{(2)}\mathrm{e}^{\frac{\mathrm{i}}{2}(\kappa^{(2)}-\kappa)}\sin\left(\frac{\kappa}{2}\right) \right]$$

$$\times \left[s_3^{(2)}\mathrm{e}^{\mathrm{i}\frac{\kappa^{(2)}}{2}} - s_3\mathrm{e}^{-\mathrm{i}\frac{\kappa}{2}} \right.$$

$$\left. -\left(s_3^{(1)}\mathrm{e}^{\mathrm{i}\frac{\kappa^{(1)}}{2}} - s_3\mathrm{e}^{-\mathrm{i}\frac{\kappa}{2}} \right) / F(\kappa^{(1)},\kappa^{(2)},\xi_j) \right]^{-1}, \quad (51)$$

where $F(\kappa^{(1)},\kappa^{(2)},\xi_j) = f(\kappa^{(1)},\xi_j)/f(\kappa^{(2)},\xi_j)$. Further we are interested in the reflection probability $|R|^2 = |R(\kappa,\xi_j)|^2$:

$$|R(\kappa,\xi_j)|^2 = \left|\left[F(\kappa^{(1)},\kappa^{(2)},\xi_j) \right.\right.$$

$$\times \left(s_3^{(2)}\mathrm{e}^{\mathrm{i}\frac{\kappa^{(2)}}{2}} - s_3\mathrm{e}^{\mathrm{i}\frac{\kappa}{2}} \right) - s_3^{(1)}\mathrm{e}^{\mathrm{i}\frac{\kappa^{(1)}}{2}} + s_3\mathrm{e}^{\mathrm{i}\frac{\kappa}{2}} \right]$$

$$\times \left[F(\kappa^{(1)},\kappa^{(2)},\xi_j)\left(s_3^{(2)}\mathrm{e}^{\mathrm{i}\frac{\kappa^{(2)}}{2}} - s_3\mathrm{e}^{-\mathrm{i}\frac{\kappa}{2}} \right) \right.$$

$$\left.\left. - s_3^{(1)}\mathrm{e}^{\mathrm{i}\frac{\kappa^{(1)}}{2}} + s_3\mathrm{e}^{-\mathrm{i}\frac{\kappa}{2}} \right]^{-1}\right|^2. \quad (52)$$

The electron transmission probability $|T(\kappa,\xi_j)|^2$ can be found from the equation

$$\left|T(\kappa,\xi_j)\right|^2 = 1 - \left|R(\kappa,\xi_j)\right|^2. \quad (53)$$

Both coefficients $|T(\kappa,\xi_j)|^2$ and $|R(\kappa,\xi_j)|^2$ are tied by the last relation and normalised to unity, thus it is enough to analyse one of them by meaning that an increase of reflection causes a decrease of transmission and vice versa.

3. Behaviour of reflection probability

3.1. Very large width of nanoribbons

For the infinite (large) width of the junction the wave vector ξ_j values change continuously and the index j is not required. At first we analyse the dependence of reflection when ξ is close to the Dirac point ($\xi = \frac{2\pi}{3}$). As shown in Fig. 3, the reflection for every κ at a certain value of the external potential sharply drops to zero, thus the junction becomes transparent for the electrons in a certain state. That state corresponds to the electron energy equal to the potential of the upper layer in bilayer graphene. Further, with increased potential, reflection increases to the maximum value and holds in a relatively wide potential range, then drops again to the lower values. Thus it is possible to control reflection (and transmission) through the barrier by external potential. The junction acts as a tunable
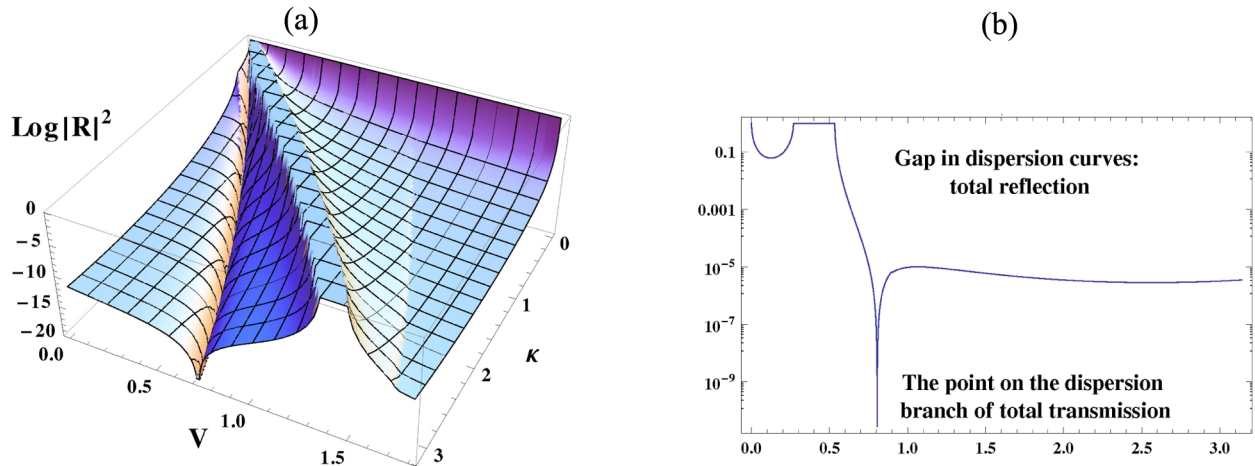

Fig. 3. (a) Dependence of reflection on the wave vector κ and the external potential V. (b) The cut of the graph in (a) at the potential $V = 0.2$.

electron spectrum filter: with certain potential we may pick which energy electrons can pass the barrier without reflection.

3.2. Finite width of nanoribbons

We have a finite number of atoms N in transverse direction, so the transverse wave vector ξ_j can obtain only certain values, numbered with the index j. These values determine the energy subbands. For the armchair bilayer graphene ribbon of infinite length with AB-α stacking, the wave vector ξ_j is determined by

$$\xi_j = \frac{\pi j}{N+1}, \qquad j = 1, \ldots, N. \tag{54}$$

In graphene and bilayer graphene nanoribbons with armchair edges the possible values of the wave vector ξ_j determine the system conductivity type, i. e. if there is an energy subband with the threshold energy coinciding with the chemical potential (which is set to zero in our investigation), the conductivity becomes metallic, otherwise bilayer graphene appears as semi-conducting. When $V = 0$ and $j^* \equiv 2(N+1)/3$ is an integer, then the armchair bilayer graphene ribbon is metallic and the index $v = j - j^* = 0$ corresponds to the zero-energy band. If $2(N+1)/3$ is not an integer, the armchair bilayer graphene ribbon spectrum has a gap, and the band closest to zero is either $j^* \equiv (2N+1)/3$ or $j^* \equiv (2N+3)/3$ depending on which of these two numbers is an integer. Thus the system with $N = 100$ is semiconducting and with $N = 101$ it is metallic. The electronic reflection (and transmission) is also affected by the width N of the nanoribbons.

By exploiting the relation (54) we show the dependence of the reflection probability on the longitudinal wave vector κ and the distance, described by the index v, from the zero energy band. It appears that the reflection probabilities for metallic nanoribbons behave similarly as those for semiconducting nanoribbons, so we show only one type in Fig. 4. As one can see, when the wave vector κ is close to zero (corresponding to the Dirac point), the reflection probability for the bands with negative and positive indices v are the same; this symmetry breaks with increasing κ. There are values of the external potential
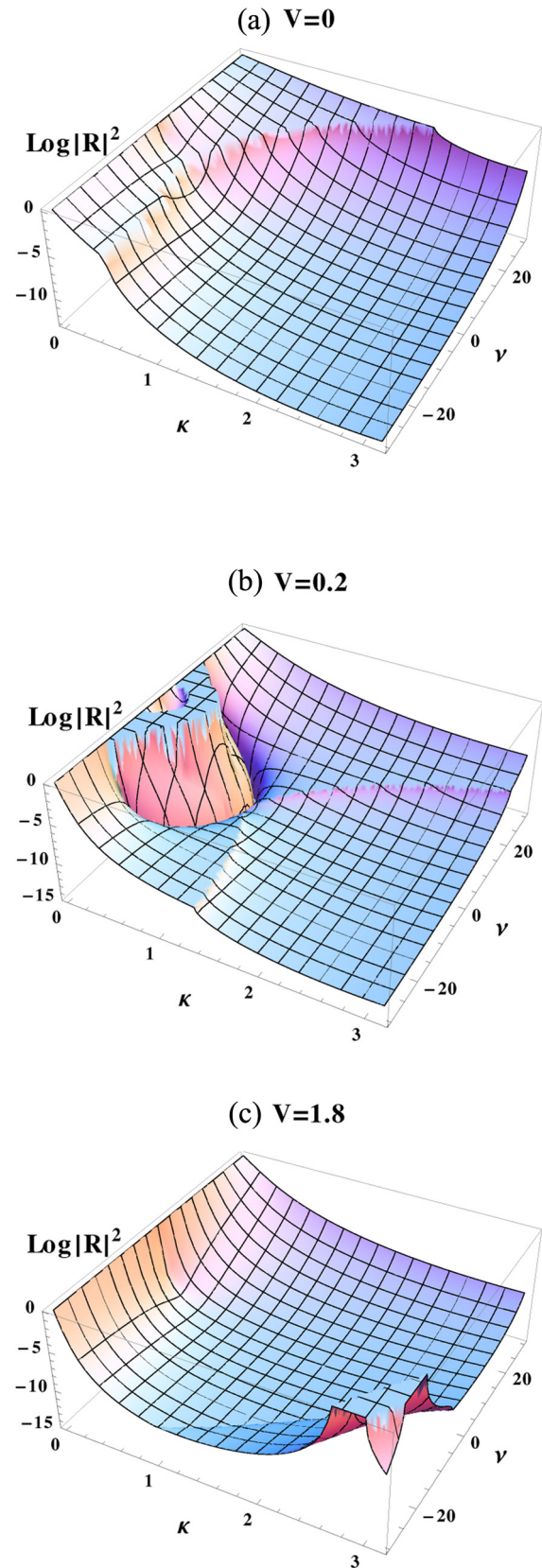

Fig. 4. Dependence of the reflection probability on the wave vector κ and the subband index v at different potentials: (a) $V = 0$, (b) $V = 0.2$, (c) $V = 1.8$.

where total transmission occurs, as can be seen in Fig. 4(b). In Fig. 4(b) the reflection probability at certain values of κ and ν drops to zero.

4. Conclusions

An exact analytical description of the electronic wave function at the graphene and AB-α stacking bilayer graphene interface based on the tight-binding model is presented. The model enables to analyse the properties of the structure far away from the Dirac point. We investigated the dependence of probabilities of electron reflection and transmission through the junction on the external voltage in bilayer graphene. We showed that transmission or reflection could be enhanced at certain voltages. This can be useful for the creation of a transistor type device from graphene nanoribbons. The model describing the system of the junction is suitable for the extension to other configurations. In addition, a finite width graphene and bilayer graphene nanoribbon junction was analysed. It was shown that the size of the ribbon affected the reflection of electrons at the junction interface. It was shown that there was no significant difference of reflection between metallic and semiconducting bilayer graphene.

References

[1] A.H.C. Neto, F. Guinea, N.M.R. Peres, K.S. Novoselov, and A.K. Geim, The electronic properties of graphene, Rev. Mod. Phys. **81**, 109 (2009).

[2] D.S.L. Abergela, V. Apalkov, J. Berashevich, K. Ziegler, and T. Chakraborty, Properties of graphene: a theoretical perspective, Adv. Phys. **59**, 261 (2010).

[3] S.D. Sarma, S. Adam, E.H. Hwang, and E. Rossi, Electronic transport in two-dimensional graphene, Rev. Mod. Phys. **83**, 407 (2011).

[4] N.M.R. Peres, Colloquium: The transport properties of graphene: An introduction, Rev. Mod. Phys. **82**, 2673 (2010).

[5] X. Du, I. Skachko, A. Barker, and E.Y. Andrei, Approaching ballistic transport in suspended graphene, Nature Nanotech. **3**, 491 (2008).

[6] E. McCann, Asymmetry gap in the electronic band structure of bilayer graphene, Phys. Rev. B **74**, 161403(R) (2006).

[7] J.B. Oostinga, H.B. Heersche, X. Liu, A.F. Morpurgo, and L.M.K. Vandersypen, Gate-induced insulating state in bilayer graphene devices, Nat. Mat. **7**, 151 (2007).

[8] F. Xia, D.B. Farmer, Y. Lin, and P. Avouris, Graphene feld-effect-transistors with high on / off current ratio, Nano Lett. **10**, 715 (2010).

[9] J. Nilsson, A. Neto, F. Guinea, and N. Peres, Transmission through a biased graphene bilayer barrier, Phys. Rev. B **76**, 165416 (2007).

[10] T. Nakanishi, M. Koshino, and T. Ando, Transmission through a boundary between monolayer and bilayer graphene, Phys. Rev. B **82**, 125428 (2010).

[11] L. Brey and H.A. Fertig, Electronic states of graphene nanoribbons studied with the Dirac equation, Phys. Rev. B **73**, 235411 (2006).

[12] H. Zheng, Z.F. Wang, T. Luo, Q.W. Shi, and J. Chen, Analytical study of electronic structure in armchair graphene nanoribbons, Phys. Rev. B **75**, 165414 (2007).

[13] L. Malysheva and A.I. Onipko, Spectrum of π electrons in graphene as a macromolecule, Phys. Rev. Lett. **100**, 186806 (2008).

[14] A. Onipko, Spectrum of π electrons in graphene as an alternant macromolecule and its specific features in quantum conductance, Phys. Rev. B **78**, 245412 (2008).

[15] L. Jiang, Y. Zheng, C. Yi, H. Li, and T. Lü, Analytical study of edge states in a semi-infinite graphene nanoribbon, Phys. Rev. B **80**, 155454 (2009).

[16] F. Guinea, A.H.C. Neto, and N.M.R. Peres, Electronic states and Landau levels in graphene stacks, Phys. Rev. B **73**, 245426 (2006).

[17] B. Partoens and F.M. Peeters, From graphene to graphite: Electronic structure around the K point, Phys. Rev. B **74**, 075404 (2006).

[18] Z.F. Wang, Q. Li, H. Su, X. Wang, Q.W. Shi, J. Chen, J. Yang, and J.G. Hou, Electronic structure of bilayer graphene: A real-space Green's function study, Phys. Rev. B **75**, 085424 (2007).

[19] J. Nilsson, A.H.C. Neto, F. Guinea, and N.M.R. Peres, Electronic properties of bilayer and multilayer graphene, Phys. Rev. B **78**, 045405 (2008).

[20] E.V. Castro, N.M.R. Peres, J.M.B.L. dos Santos, A.H.C. Neto, and F. Guinea, Localized States at zigzag edges of bilayer graphene, Phys. Rev. Lett. **100**, 026802 (2008).

[21] J. Ruseckas, G. Juzeliūnas, and I.V. Zozoulenko, Spectrum of π electrons in bilayer graphene nanoribbons and nanotubes: An analytical approach, Phys. Rev. B **83**, 035403 (2011).

[22] H. Xu, T. Heinzel, and I.V. Zozoulenko, Edge disorder and localization regimes in bilayer graphene nanoribbons, Phys. Rev. B **80**, 045308 (2009).

[23] H. Xu, T. Heinzel, A.A. Shylau, and I.V. Zozoulenko, Interactions and screening in gated bilayer graphene nanoribbons, Phys. Rev. B **82**, 115311 (2010).

ELEKTRONŲ PRALAIDUMO GRAFENO IR BIGRAFENO SANDŪROJE ANALIZINIS ARTINYS

J. Ruseckas [a], A. Mekys [a], G. Juzeliūnas [a, b], I.V. Zozoulenko [c]

[a] *Vilniaus universiteto Teorinės fizikos ir astronomijos institutas, Vilnius, Lietuva*
[b] *Lietuvos edukologijos universitetas, Vilnius, Lietuva*

[c] *Linčiopingo universitetas, Norčiopingas, Švedija*

Santrauka

Grafenas – tai lakštas, sudarytas iš anglies atomų, išsidėsčiusių plokštumoje heksagonine struktūra. Nuo 2004 m. juo susidomėta dėl specifinių elektronų pernašos savybių. Buvo nustatyta, kad krūvininkų judris (kambario temperatūroje) jame didžiausias iš visų iki šiol žinomų medžiagų, o IBM firma jau pademonstravo veikiantį lauko tranzistorių, pagamintą iš dvigubo grafeno sluoksnio. Grafenas yra pusmetalis, neturintis draustinių energijų tarpo, o ties Fermi energija būsenų tankis lygus nuliui. Draustinių energijų tarpas yra reikalingas atlikti tranzistoriaus valdymo funkcijas. Bigrafene šis tarpas sukuriamas prijungus įtampą tarp sluoksnių, o grafene, pasirodo, jis atsiranda, kai grafeno lakštas sumažinamas iki nanojuostos matmenų. Grafeno ir bigrafeno banginės funkcijos jau buvo suskaičiuotos anksčiau artimo ryšio metodu. Šiame darbe buvo pasinaudota jau turimais sprendiniais ir suskaičiuota nauja grafeno ir AB-α konfigūracijos bigrafeno barjerinės sandūros būsenos funkcija, su kuria pavyko analiziškai užrašyti elektrono pralaidumo per sistemą ir atspindžio tikimybes, išreikštas elementariomis funkcijomis. Ši struktūra yra asimetrinio lauko tranzistoriaus atitikmuo, kuriame užtūrą sudaro viršutinis grafeno lakštas bigrafene. Veikiant išoriniu elektriniu lauku, galima valdyti elektronų pralaidumą per sistemą. Tokios pat sandaros sitema jau buvo nagrinėta ir anksčiau, tačiau tik tolydiniu artiniu, o pateikti dėsningumai nėra pakankamai išanalizuoti. Šiame darbe suskaičiuota atspindžio tikimybės priklausomybė nuo išorinio potencialo tarp bigrafeno sluoksnių ir nuo banginio vektoriaus. Nustatyta, kad potencialui didėjant atspindys rezonansiškai išauga iki maksimalios vertės (absoliutaus atspindžio), tada krinta iki minimalios (absoliutaus pralaidumo), t. y. galima tokią sistemą valdyti išoriniu potencialu. Taip pat nustatyta, kaip keičiasi sistemos savybės, kai grafeno ir bigrafeno sandūra pagaminama ant baigtinio pločio nanojuostos.